Neurobiology of Disease 174 (2022) 105860

Contents lists available at ScienceDirect

Neurobiology of Disease

journal homepage: www.elsevier.com/locate/ynbdi

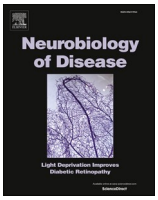

Epilepsy phenotype and response to KCNQ openers in mice harboring the *Kcnq2* R207W voltage-sensor mutation

Fuyun Tian [a,b,c], Birong Cao [a,b,c], Haiyan Xu [b], Li Zhan [b], Fajun Nan [b], Ning Li [e,f], Maurizio Taglialatela [d,**], Zhaobing Gao [a,b,c,*]

[a] Zhongshan Institute of Drug Discovery, Shanghai Institute of Materia Medica, Chinese Academy of Science, Zhongshan, Guangdong, China
[b] Center for Neurological and Psychiatric Research and Drug Discovery, Shanghai Institute of Materia Medica, Chinese Academy of Sciences, Shanghai, China
[c] University of Chinese Academy of Sciences, Beijing, China
[d] Department of Neuroscience, University of Naples "Federico II", 80131 Naples, Italy
[e] Division of Life Science, The Hong Kong University of Science and Technology, Hong Kong, China
[f] HKUST Shenzhen Research Institute, 518057 Shenzhen, China

ARTICLE INFO

Keywords:
KCNQ2
Epilepsy
Mouse model
HN37 (pynegabine)

ABSTRACT

KCNQ2-encoded Kv7.2 subunits play a critical role in balancing neuronal excitability. Mutations in KCNQ2 are responsible for highly-heterogenous epileptic and neurodevelopmental phenotypes ranging from self-limited familial neonatal epilepsy (SeLFNE) to severe developmental and epileptic encephalopathy (DEE). Pathogenic KCNQ2 variants cluster at the voltage sensor domain (VSD), the pore domain, and the C-terminal tail. Although several knock-in mice harboring *Kcnq2* pore variants have been developed, no mouse line carrying *Kcnq2* voltage-sensor mutations has been described. KCNQ2-R207W is an epilepsy-causing mutation located in the VSD, mainly affecting voltage-dependent channel gating. To study the physiological consequence of *Kcnq2* VSD dysfunction, we generated a *Kcnq2*-R207W mouse line and analyzed the pathological and pharmacological phenotypes of mutant mice. As a result, both homozygous ($Kcnq2^{RW/RW}$) and heterozygous ($Kcnq2^{RW/+}$) mice were viable. While $Kcnq2^{RW/RW}$ mice displayed a short lifespan, growth retardation, and spontaneous seizures, $Kcnq2^{RW/+}$ mice survived and developed normally, although only a fraction (9/64; 14%) of them showed behavioral- and ECoG-confirmed spontaneous seizures. $Kcnq2^{RW/+}$ mice displayed increased susceptibility to evoked seizures, which was dramatically ameliorated by treatment with the novel KCNQ opener pynegabine (HN37). Our results show that the *Kcnq2*-R207W mouse line, the first harboring a *Kcnq2* voltage-sensor mutation, exhibits a unique epileptic phenotype with both spontaneous seizures and increased susceptibility to evoked seizures. In *Kcnq2*-R207W mice, the potent KCNQ opener HN37, currently in clinical phase I, shows strong anticonvulsant activity, suggesting it may represent a valuable option for the severe phenotypes of KCNQ2-related epilepsy.

1. Introduction

KCNQ2 subunits, the main molecular components of the M channel, play diverse roles in regulating neuronal excitability, including spike frequency adaption (Brown and Adams, 1980), afterhyperpolarization (Martire et al., 2004), and modulation of transmitter release (Martire et al., 2004; Uchida et al., 2017). Human genetic variants in the KCNQ2 gene cause epilepsy (Miceli et al., 2010); in fact, the KCNQ2 gene was first identified and cloned in families affected with self-limited familial neonatal epilepsy (SeLFNE, OMIM #121200) (Biervert et al., 1998; Singh et al., 1998), an autosomal dominant disease characterized by frequent seizures occurring in the first few days of life spontaneously

Abbreviations: KCNQ2, Potassium Voltage-Gated Channel Subfamily Q Member 2; SeLFNE, Self-limited familial neonatal epilepsy; DEE7, Developmental and epileptic encephalopathy 7; LOF, Loss-of-function; VSD, Voltage-sensor domain; ECoG, Electrocorticography; GTCS, Generalized tonic-clonic seizures; SUDEP, Sudden unexpected death in epilepsy; ASM, Anti-seizure medication.

* Correspondence to: Z Gao, Center for Neurological and Psychiatric Research and Drug Discovery, Shanghai Institute of Materia Medica, Chinese Academy of Sciences, 555 Zuchongzhi Road, Shanghai 201203, China.
** Correspondence to: M Taglialatela, Department of Neuroscience, University of Naples "Federico II", 80131 Naples, Italy.
E-mail addresses: mtaglial@unina.it (M. Taglialatela), zbgao@simm.ac.cn (Z. Gao).

https://doi.org/10.1016/j.nbd.2022.105860
Received 3 July 2022; Received in revised form 7 September 2022; Accepted 12 September 2022
Available online 14 September 2022

disappearing after a few weeks or months, with generally normal neuropsychological development. In addition, a wide spectrum of more severe epileptic phenotypes have been recognized as results of pathogenic variants in KCNQ2, including developmental and epileptic encephalopathy (DEE7, OMIM #613720), a disease characterized by early-onset refractory seizures, neuroradiological alterations, and developmental delay (Miceli et al., 2010; Weckhuysen et al., 2012). Mutations in KCNQ2 are the most frequent cause of neonatal-onset genetically-determined epilepsies(Symonds et al., 2019).

In order to study the pathogenetic mechanisms and potential therapeutic strategies of KCNQ2-related epilepsy, several mouse models of KCNQ2 dysfunction have been developed. The first is the *Kcnq2*-knockout mice generated by homologous recombination; while homozygous pups died in the first postnatal day from pulmonary atelectasis, heterozygous mice showed increased susceptibility to seizure in spite of their normal morphology and behavior (Watanabe et al., 2000). Unlike *Kcnq2*-knockout mice, mice with a conditional dominant-negative human *KCNQ2*-G279S transgene exhibited spontaneous seizures, memory impairment, and neuropathological changes, but the genotype of these transgenic mice was different from that of patients, who typically carry the disease-causing mutations in heterozygosity (Peters et al., 2005). To overcome this limitation, knock-in mice carrying the *Kcnq2* loss-of-function (LOF) mutations A306T or Y284C were developed (Singh et al., 2008; Tomonoh et al., 2014). The two mouse models, *Kcnq2*-A306T and *Kcnq2*-Y284C, expressed somewhat similar phenotypes, with homozygous mice of both lines displaying spontaneous seizures and heterozygous mice showing increased susceptibility to induced seizures but no spontaneous seizure activity (Otto et al., 2009; Singh et al., 2008; Tomonoh et al., 2014). More recently, a mouse model (*Kcnq2*-T274M) knock-in for one of the most recurrent disease-causing variants in humans has been reported; notably, heterozygous *Kcnq2*-T274M animals, maintained in the 129Sv genetic background, displayed spontaneous seizures (Milh et al., 2020). Collectively, all knock-in mouse models above carry mutations in the pore-forming region of the KCNQ2 subunit (Fig. 1A), while no reports are available of mice models harboring *Kcnq2* mutations in the S4 voltage sensor, a critical region for channel function and a mutational hotspot in KCNQ2-related epilepsies.

R207W is a pathogenic mutation that abolishes the third of six positive charges in the S4 transmembrane segment of the voltage-sensor domain (VSD) of the KCNQ2 subunit; the mutation is responsible for a wide spectrum of epileptic phenotypes, including SeLFNE, DEE7, and myokymia (Blumkin et al., 2012; Dedek et al., 2001; Dhamija et al., 2017; Soldovieri et al., 2014). KCNQ2 subunits carrying the substitution of the positively charged arginine at position 207 with a bulky hydrophobic residue exert dominant-negative loss-of-function effects when expressed in vitro by shifting the voltage dependence of channel activation to a more positive voltage and slowing channel activation, which could be rescued by KCNQ opener (Xiong et al., 2007; Xiong et al., 2008); similar, although less dramatic, gating consequences occurred when the R207 residue was replaced by a neutral glutamine (R207Q) (Miceli et al., 2008). In Kv7.4 channels highly functionally and structurally related to Kv7.2, mutations corresponding to R207W and R207Q in Kv7.2 generated nonlinear currents with complex kinetics after ionic current suppression; the biophysical and pharmacological characteristics of these currents were consistent with those of the so-called ω-currents, namely currents carried through water-filled regions of the protein (crevices or gating pores) created by specific conformations of the VSD, rather than through the canonical pore (Miceli et al., 2012). Recent results using atom-detailed molecular dynamics simulations and a refined model structure of the Kv7.2 VSD in the active conformation further showed that the R207Q mutation significantly increases the

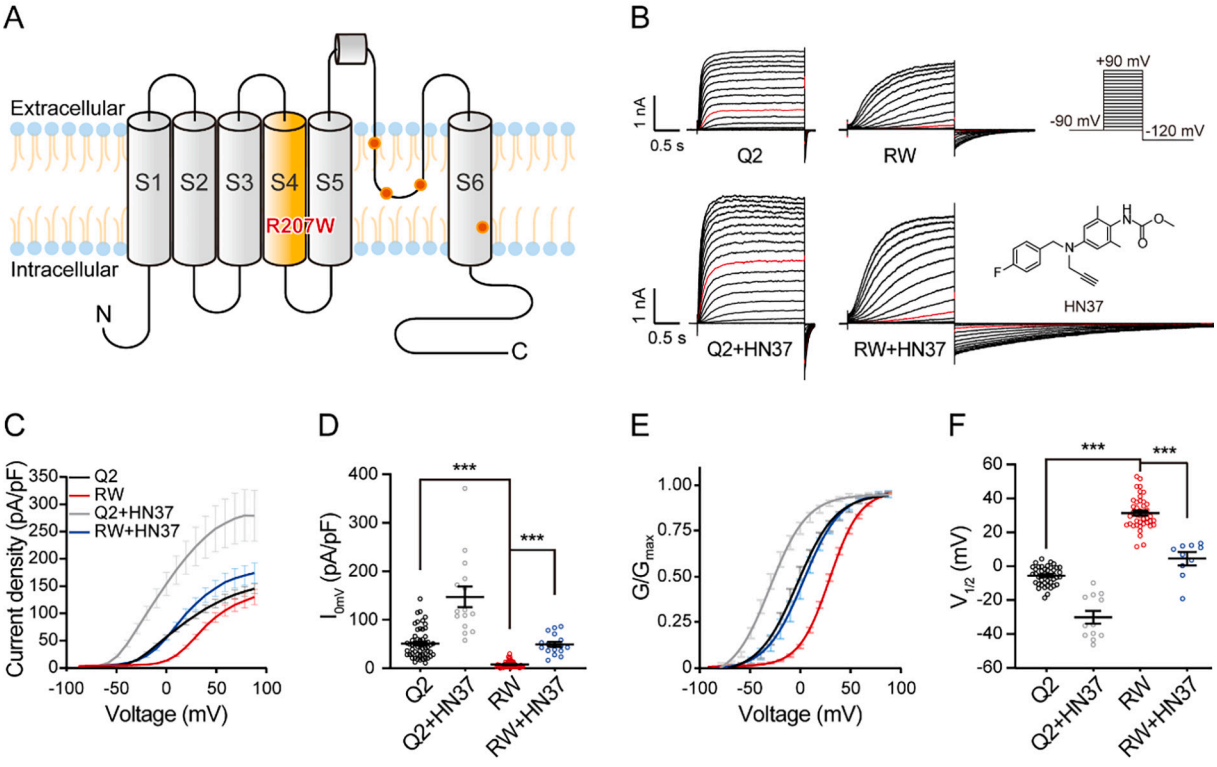

Fig. 1. The location and electrophysiological phenotype of KCNQ2 mutation R207W.
A) Distribution of R207W and other published variants (T274M, G279S, Y284C and A306T) within KCNQ2 subunit. B) Representative current traces of KCNQ2 (Q2) and R207W (RW) mutant before and after application of 100 nM HN37. Currents were elicited by depolarization from −90 mV to +90 mV in 10 mV incremental steps from holding potential −90 mV. C) Current density-voltage curve and D) Current at 0 mV of KCNQ2 and R207W mutant before and after application of 100 nM HN37. E) G-V curve and F) $V_{1/2}$ of KCNQ2 and R207W mutant before and after application of 100 nM HN37.

hydration in the internal VSD cavity, a feature favoring the occurrence of ω-currents (Alberini et al., 2021).

In order to assess the in vivo consequences of the R207W mutation in the VSD of KCNQ2, we developed a *Kcnq2*-R207W mouse line and analyzed the epilepsy phenotypes of both homozygous (*Kcnq2*$^{RW/RW}$) and heterozygous (*Kcnq2*$^{RW/+}$) mutants. In addition, we tested the anticonvulsant effects of the novel KCNQ opener HN37 (Zhang et al., 2021) in *Kcnq2*$^{RW/+}$ mice. We report that HN37 protects *Kcnq2*$^{RW/+}$ mice against induced seizures in vivo, suggesting the potential usefulness of this drug as a precision strategy for treating the severe forms of KCNQ2-related disorders.

2. Materials and methods

2.1. Cell culture and transient transfection

KCNQ subunits were expressed in CHO cells grown in DMEM/F12 (1:1) supplemented with 10% FBS. Twenty-four hours before electrophysiological recording, cells were transiently transfected with Lipofectamine 3000 reagent (Invitrogen). A plasmid encoding EGFP was used as a transfection marker, and total cDNA in the transfection mixture was kept constant at 4 μg.

2.2. Electrophysiological recording

KCNQ2 channel currents were recorded at room temperature using standard whole-cell patch clamping; data acquisition was performed using an Axopatch-700B amplifier, with the signals filtered at 2 kHz and digitized with a Digidata 1440 A interface at 50 kHz. Pipettes of 2–5 MΩ resistance when filled with the intracellular solution were used. The pipette solution contained 145 mM KCl, 1 mM $MgCl_2$, 1 $CaCl_2$, 5 mM EGTA, and 10 mM HEPES (pH 7.2 adjusted by KOH); the extracellular solution contained 140 mM NaCl, 5 mM KCl, 2 mM $CaCl_2$, 1 mM $MgCl_2$, 10 mM Glucose and 10 mM HEPES (pH 7.4 adjusted by NaOH). During the recordings, constant perfusion of the extracellular solution was maintained using a BPS perfusion system (ALA Scientific). Normalized conductance-voltage (G-V) relationships were fitted using the Boltzmann equation. Data analysis was performed using CLAMPFIT 9 (Axon Instruments) and GraphPad Prism 8.

2.3. Animals

All experiments involving animals were performed in accordance with the National Institutes of Health Guide for the Care and Use of Laboratory Animals. Animal protocols were approved by the IACUC (Institutional Animal Care and Use Committees) and were carried out following the approved guidelines. Knock-in mice with *Kcnq2*-R207W variant on C57BL/6 J background were from Shanghai Model Organisms, and an off-target analysis was performed and no hits in any of the potential off-target sites screened were identified. The F1 generations were backcrossed at least five generations with wild-type C57BL/6 J to eliminate possible unwanted off-target effects. All mice used in this work were obtained by breeding *Kcnq2*$^{RW/+}$ males with *Kcnq2*$^{RW/+}$ females, and offspring mice were genotyped by PCR of tail biopsy DNA. For amplification, Primer 1, ACACTACAGGTAGGCAGGGTGG; primer 2, GCTCCAGGAAGGATTGCTCACA; Primer 1 was used for sequencing. KCNQ2 protein expression in mice brain was determined by Western blot analysis (Supplementary Material). Mice were housed in a specific pathogen-free barrier facility with a 12/12-h light/dark cycle and had ad libitum access to food and water. Male mice were used for the study.

2.4. Open-field test

Mice locomotor activity was measured using an open field test in a dark environment. Each mouse was placed in the same corner of the open field apparatus (50 × 50 × 40 cm), then the spontaneous locomotor activity of each mouse was monitored by an infrared-sensitive camera and analyzed with an automated tracking system (Shanghai Xinsoft Information Technology, Shanghai, China). Data were collected for 10 min for each mouse.

2.5. ECoG analysis

Mice (P56-P70) were anesthetized using isoflurane and fixed to a stereotaxic stage. After midline skin incisions, the skull was exposed and cleaned with hydrogen peroxide. The skull was drilled with a 1 ml syringe needle, and isolated pin headers were inserted (subdural 1.0 mm) as electrodes for ECoG. The recording electrode was implanted 2 mm posterior to bregma and 2 mm right to the midline; the reference electrode was implanted 3 mm anterior to bregma and 2 mm left to the midline, and the ground electrode was implanted on the skull over the cerebellum. Then the electrodes were fixed to the skull with 502 glue (an ethyl-cyanoacrylate-based glue) and dental cement. At least 5 days after surgery, digital ECoG activity was monitored in each mouse for 5 days using the RM6280 system (Chengdu Instrument Factory, Chengdu, China) or Medusa system (Bio-Signal Technologies, Nanjing, China). All recordings were carried out on mice freely moving in the test cage; infrared-sensitive video cameras were used to monitor locomotor activity during the ECoG recording periods.

2.6. Drugs

Pynegabine (HN37) and retigabine (RTG) were provided by Dr. Fajun Nan (National Center for Drug Screening, Chinese Academy of Sciences, Shanghai, China). Pentylenetetrazole (PTZ), sodium carboxymethyl cellulose (CMC—Na), and NaCl were from Sigma-Aldrich (USA). For the antiepileptic activity test in *Kcnq2*$^{RW/+}$, HN37 and RTG were suspended in 0.5% CMC-Na and administered intragastrically to experimental mice in a volume of 20 ml/kg, and the seizure test was performed 1 h after administration. PTZ was solubilized in normal saline.

2.7. Seizure induction

Induction of audiogenic seizure. The sound-proof chamber was made of transparent Plexiglas and could be opened and covered from the top. The noise was provided by a speaker mounted on the ceiling of the chamber. Male mice (P28-P35) of different genotypes were placed into the chamber and habituated for a 1-min period. Then mice were subjected to a 110 dB noise for 1 min, or until generalized tonic-clonic seizures (GTCS) occurred. GTCS number and latencies were analyzed after testing.

Hyperthermia-induced seizure test. Male mice (P35-P42) of *Kcnq2*$^{RW/+}$ and WT genotypes were used in the hyperthermia-induced seizures test. Before seizure induction, the body temperature of mice was measured by a rectal probe (TCAT 2DF, Physitemp, USA), and the core temperature of different groups was maintained at approximately 36.5 °C. Mice were placed into an electric heating constant temperature incubator (Zhicheng, Shanghai) with a temperature of 50 °C to determine seizure susceptibility of *Kcnq2*$^{RW/+}$ and WT mice to hyperthermia or to evaluate the effectiveness of the test anti-seizure medications (ASMs) in *Kcnq2*$^{RW/+}$ mice. The behaviors of mice were observed through a transparent window; mice were kept in the incubator until GTCS occurred but not longer than 10 min, and then the body temperature of each mouse was immediately measured by the rectal probe. The time and body temperature when GTCS occurred were recorded in these experiments.

Maximal electroshock seizure (MES) test. Mice (P42-P56) of *Kcnq2*$^{RW/+}$ and WT genotypes were used in the MES test. The electrical shock was delivered by an electronic stimulator (EC-02, Orchid Scientifics, Maharashtra, India) by the delivery of a current of 0.25 to 10 mA (continuous sinusoidal wave with a frequency of 0.5 Hz, a wave width of 0.2 ms) for 0.2 s through ear clip. Mice were scored for the presence or absence of

immediate tonic hindlimb extension.

6-Hz psychomotor seizure test. An electrical stimulus was delivered through corneal electrodes to male mice (P42-P56) of *Kcnq2*$^{RW/+}$ and WT genotypes, which is pre-treated with saline diluted with 0.5% tetracaine hydrochloride for local anesthesia and to improve electrical conductivity; a Grass electronic stimulator (S48, Grass Technologies, USA) was used with a constant current unit (CCU1, Grass Technologies, USA) to determine seizure susceptibility of *Kcnq2*$^{RW/+}$ and WT mice or to evaluate the effectiveness of the test ASMs in *Kcnq2*$^{RW/+}$ mice. For antiepileptic activity evaluation, the seizures were induced by a stimulus of 20 mA current (6-Hz, 0.2 ms rectangular pulse width) for 3 s duration. The ED_{50} values of HN37 and RTG were evaluated by non-linear regression using GraphPad Prism (GraphPad Software, USA).

Subcutaneous PTZ (sc-PTZ) test. PTZ was injected subcutaneously into male mice (P42-P56) of *Kcnq2*$^{RW/+}$ and WT genotypes. The proportion and the latency of GTCS were recorded within 1 h after PTZ application to determine seizure susceptibility of *Kcnq2*$^{RW/+}$ and WT mice or to evaluate the effectiveness of the test ASMs in *Kcnq2*$^{RW/+}$ mice. For antiepileptic activity evaluation, PTZ was injected at a dose of 60 mg/kg body weight. Seizures were scored based on convulsive behavior using the following version of the Racine's scale: Stage I, facial or mouth twitching; stage II, Head nodding, myoclonic jerk; stage III, unilateral forelimb clonus; stage IV, bilateral forelimb clonus with rearing and falling, wild running and jumping; stage V, falling with tonic-clonic seizures; and stage VI, hind limb tonic extension and death.

2.8. Statistics

The data are shown as the mean ± SEM, and the significance was estimated using the Student's *t*-test unless otherwise stated. Statistical significance: * $p \leq 0.05$, ** $p \leq 0.01$, *** $p \leq 0.001$.

3. Results

3.1. Functional and pharmacological characterization of KCNQ2 channels carrying the R207W mutation

The epilepsy-causing KCNQ2-R207W variant neutralizes the third positively-charged amino acid in the S4 segment in the VSD (Fig. 1A). In our expression system in CHO-K1 cells, R207W mutant channels exhibited a distinct loss-of-function (LOF) electrophysiological phenotype, including slower activation kinetics, decreased current density at physiological membrane potentials, and a rightward shift of the G-V relationship (Fig. 1B). At a membrane potential of 0 mV, the current

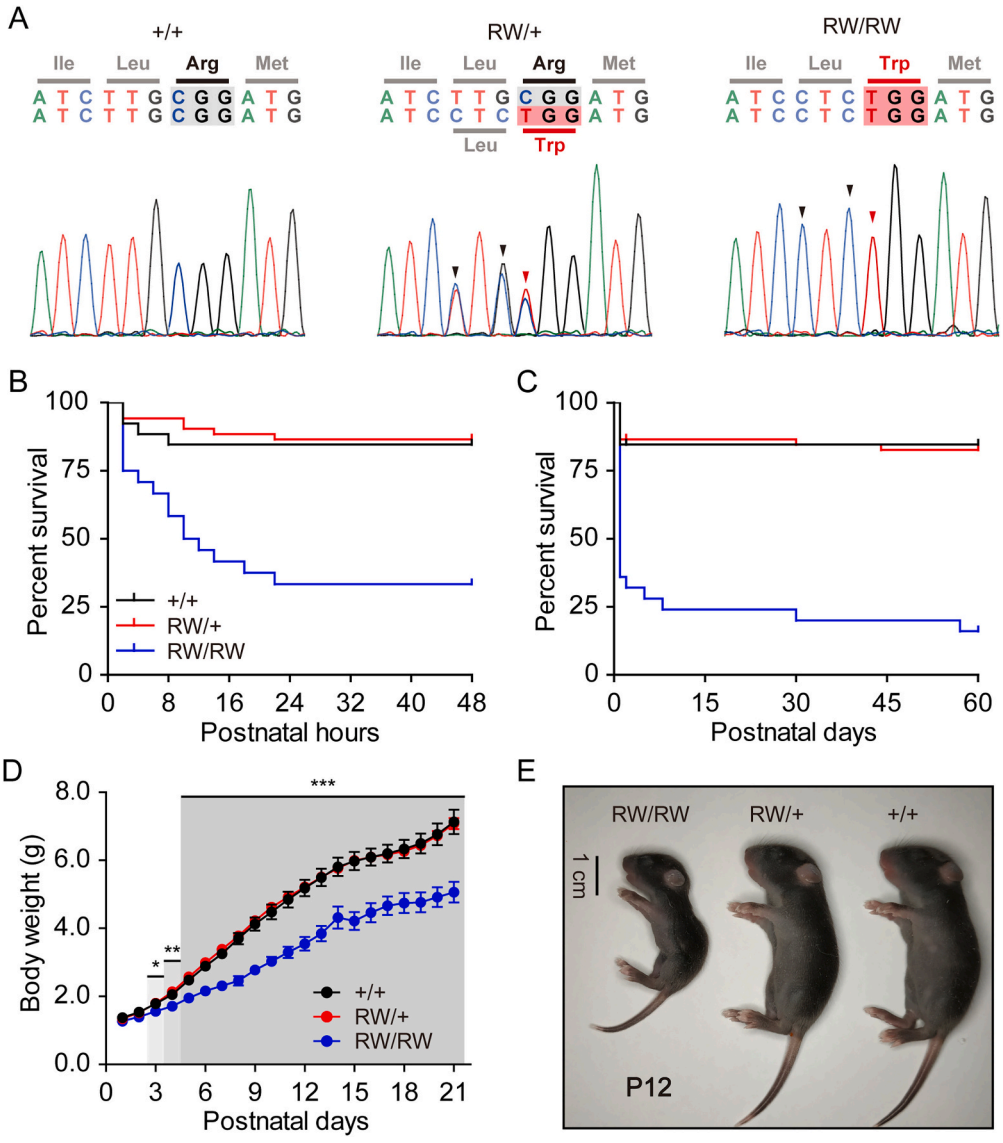

Fig. 2. The survival and growth of *Kcnq2*-R207W mice.
A) Nucleotide sequence of WT, *Kcnq2*$^{RW/+}$ and *Kcnq2*$^{RW/RW}$ mice. In the *Kcnq2*-R207W mice constructed, nucleotide changes were presented at three positions in mutant allele, the c.619C > T lead to p. Arg207Trp while the two others were synonymous mutations. While synonymous mutated bases are marked by black arrowheads, missense mutated base (c.619C > T) are marked by red arrowheads., Life span of *Kcnq2*$^{RW/RW}$ *Kcnq2*$^{RW/+}$ and WT mice monitored for a B) 48-h or C) 60-day period; n = 20–60 per group; p<0.001 for WT vs. HO, log-rank test. D) The weight gain of *Kcnq2*$^{RW/RW}$, *Kcnq2*$^{RW/+}$ and WT mice monitored for a 21-day period; n = 20–60 per group. E) The body size of *Kcnq2*$^{RW/RW}$, *Kcnq2*$^{RW/+}$ and WT mice in P12. (For interpretation of the references to colour in this figure legend, the reader is referred to the web version of this article.)

density was significantly smaller in R207W when compared to WT channels (12.84 ± 2.46 pA/pF vs. 39.76 ± 7.73 pA/pF)($p < 0.0001$, Student's *t*-test) and increased to 65.60 ± 10.32 pA/pF after application of 100 nM of the KCNQ opener HN37 ($p < 0.0001$, Student's t-test) (Fig. 1C, D). In addition, when compared to WT channels, R207W mutant channels showed a more depolarized half-activation voltage (29.05 ± 3.21 mV vs.4.79 ± 2.36 mV) ($p < 0.0001$, Student's t-test), which could be largely rescued to WT values by the application of 100 nM HN37 ($p < 0.0001$, Student's t-test) (Fig. 1E, F). Considering its location in the VSD and its unique electrophysiological characteristics when expressed in vitro, we chose the R207W variant to develop a novel mouse model of KCNQ2-related epilepsy.

3.2. Homozygous *Kcnq2*$^{RW/RW}$ mice display early death and developmental delay

We generated a knock-in mouse model carrying a *Kcnq2* mutation R207W using the CRISPR/Cas9 system, in which the third positively-charged arginine residue in the S4 segment was substituted with a tryptophan residue (c.619C > T leads to p.Arg207Trp) (Fig. 2A). To assess the viability of homozygous (*Kcnq2*$^{RW/RW}$) and heterozygous (*Kcnq2*$^{RW/+}$) mutants, we carried out crosses between *Kcnq2*$^{RW/+}$ mice, and offsprings were genotyped by PCR amplification and DNA sequencing (Fig. 2A). We found that both heterozygous and homozygous mutants were viable, and the yield of wild-type (*Kcnq2*$^{+/+}$) (26), *Kcnq2*$^{RW/+}$ (51), and *Kcnq2*$^{RW/RW}$ (25) pups was consistent with the predicted Mendelian ratio of 1:2:1.

Most *Kcnq2*$^{RW/RW}$ mice (16/25; 64%) died within 48 h after birth, and only 4 out of 25 homozygotes (16%) survived to weaning (Fig. 2B, C). The surviving homozygous *Kcnq2*$^{RW/RW}$ mice showed gait abnormality and weakness between the second and fourth weeks of life, also exhibiting a severe growth delay across the lifespan since postnatal day 3 (P3) (Fig. 2D), with abnormal size and appearance (Fig. 2E). Despite such a severe phenotype, the reproductive capacity was retained in *Kcnq2*$^{RW/RW}$ homozygous mice, and multiple crosses between surviving mice were performed. Instead, unlike homozygous mutant mice, heterozygous *Kcnq2*$^{RW/+}$ mice appeared normal in their survival rate, size, and appearance and gained weight at a rate similar to age-matched *Kcnq2*$^{+/+}$ littermates (Fig. 2).

3.3. Spontaneous seizure phenotype in homozygous and heterozygous mice carrying the R207W mutation

Continuous video recordings were performed to monitor seizure behaviors in *Kcnq2*-R207W mutants. *Kcnq2*$^{RW/RW}$ mice exhibited spontaneous seizures, including myoclonic, generalized tonic-clonic seizures (GTCS), leading eventually to sudden unexpected death in epilepsy (SUDEP); all cases of premature death of adult *Kcnq2*$^{RW/RW}$ mice were observed following single or recurrent GTCS (Supplementary Video 1). Considering that patients carrying the KCNQ2-R207W variant are heterozygous and that *Kcnq2*$^{RW/RW}$ mice are too weak to bear the electrode implantation surgery, we did not perform further electrocorticographic (ECoG) recordings in *Kcnq2*$^{RW/RW}$ mice.

Instead, only 14% (9/64) of heterozygous *Kcnq2*$^{RW/+}$ mice aged from 6 weeks to 10 weeks showed apparent behavioral signs of seizures, including wild running, circling, myoclonus, GTCS, and also SUDEP; this result suggests incomplete penetrance of the spontaneous seizure phenotype in adult *Kcnq2*$^{RW/+}$ mice. *Kcnq2*$^{+/+}$ and *Kcnq2*$^{RW/+}$ mice aged 8 to 10 weeks were then implanted with epidural electrodes for continuous ECoG recordings with simultaneous video monitoring. During 120-h recordings, several *Kcnq2*$^{RW/+}$ mice (3/16) exhibited severe epileptic discharges, accompanied by GTCS and even SUDEP, while no WT mice displayed spontaneous seizures (Fig. 3A, B). A representative ictal ECoG trace recorded from one heterozygous mouse is shown in Fig. 3A, which was distinguishable from the ECoG recording of the *Kcnq2*$^{+/+}$ mice. The accompanying behavioral seizure is shown in Supplementary Video 2; in this video, it could be observed the animal having myoclonus, wild running, and GTCS, and, after a few seconds, falling down with a rigid posture; at this time, the ECoG flattened (Fig. 3A). The three *Kcnq2*$^{RW/+}$ mice with spontaneous seizures investigated all suffered from recurrent seizures 7.33 ± 3.93 times/day, and the averaged seizure duration was 25.65 ± 5.23 s (Fig. 3C, D).

Although *Kcnq2*$^{RW/+}$ mice displayed only an incomplete penetrance of spontaneous seizures, they all showed hyperexcitable phenotypes when housed in their home cage since two weeks after birth, including increased locomotor activity, excessive jumping, and exaggerated startle responses compared to *Kcnq2*$^{+/+}$ mice. Therefore, a better assessment of locomotor activity in these mice was performed in the open-field test. During the observation period, a marked increase in the total distance covered was observed in *Kcnq2*$^{RW/+}$ mice when compared to *Kcnq2*$^{+/+}$ mice ($p < 0.0001$, Student's *t*-test), with a significant decrease in immobility time in *Kcnq2*$^{RW/+}$ mice ($p = 0.0013$, Student's t-test) (Fig. 3F, G).

3.4. Heterozygous mice displayed heightened seizure susceptibility to noise and hyperthermia compared to wild-type mice

Kcnq2-R207W mice appeared hypersensitive to various disturbances such as fighting, cage changing, or sudden noise. To evaluate the sensitivity to audiogenic stimuli in mutants, we tested the epileptic behavior of *Kcnq2*$^{RW/+}$ and *Kcnq2*$^{+/+}$ mice (4–5 weeks of age) when subjected to a 110-dB sound stimulus. After exposure to the noise, 30% (6/20) of *Kcnq2*$^{RW/+}$ mice tested showed a severe SUDEP phenotype within 30 s, while no *Kcnq2*$^{+/+}$ mice (0/12) exhibited epileptic seizures (Fig. 4A), suggesting an increased susceptibility to audiogenic seizures in *Kcnq2*$^{RW/+}$ mice ($p = 0.0353$, Chi-square test).

The severity of seizure symptoms increased with fever in some reported cases of KCNQ2-related epilepsy (Dedek et al., 2001; Dhamija et al., 2017); thus, we evaluated the seizure susceptibility to hyperthermia in *Kcnq2*$^{RW/+}$ mice. The mice were kept inside an incubator with a constant temperature of 50 °C for 10 min or until a GTCS occurred, and then the GTCS latency and body temperature were measured immediately using a rectal temperature probe. The GTCS in *Kcnq2*$^{RW/+}$ mice occurred significantly earlier than in *Kcnq2*$^{+/+}$ mice (330.30 ± 16.61 s vs. 410.40 ± 30.94 s) ($p < 0.0001$, Student's t-test), and GTCS in *Kcnq2*$^{RW/+}$ mice occurred at an average temperature of 43.52 ± 0.14 °C, a value markedly lower than that recorded in WT mice (44.79 ± 0.21 °C)($p = 0.0125$, Student's t-test) (Fig. 4B, C), indicating that *Kcnq2*$^{RW/+}$ mice were more susceptible to seizures induced by hyperthermia when compared to *Kcnq2*$^{+/+}$ mice.

3.5. *Kcnq2*$^{RW/+}$ mice displayed heightened seizure susceptibility to electrical and chemical stimuli compared to wild-type mice

In addition to noise and hyperthermia, the susceptibility of *Kcnq2*$^{RW/+}$ mice to electrically-induced seizures was determined using the maximal electroshock seizure (MES) model. As shown in Fig. 4D, the current strength needed to evoke tonic hind limb extension in 50% of the animals tested (CS_{50}, expressed in mA) of *Kcnq2*$^{RW/+}$ (0.47 mA) was markedly lower than that needed to evoke the same response in *Kcnq2*$^{+/+}$ mice (2.16 mA), suggesting a significant MES threshold decrease in *Kcnq2*$^{+/+}$ mice ($p = 0.0152$, two-way ANOVA, Bonferroni test).

The 6-Hz seizure test was then employed using various intensities of stimulation currents. As shown in Fig. 4E, when compared to WT mice, the seizure rate curve of *Kcnq2*$^{RW/+}$ mice showed a visible leftward shift ($p = 0.0305$, two-way ANOVA, Bonferroni test). As shown in Fig. 4F, seizure duration in *Kcnq2*$^{RW/+}$ mice at each stimulus intensity was markedly longer than that of *Kcnq2*$^{+/+}$ mice at 15 mA or 20 mA ($p = 0.0002$ and $p < 0.0001$, one-way ANOVA, Turkey's multiple comparison test); moreover, while *Kcnq2*$^{RW/+}$ mice generally exhibited GTCS, *Kcnq2*$^{+/+}$ mice only showed partial seizures.

To investigate possible differences between *Kcnq2*$^{RW/+}$ and *Kcnq2*$^{+/}$

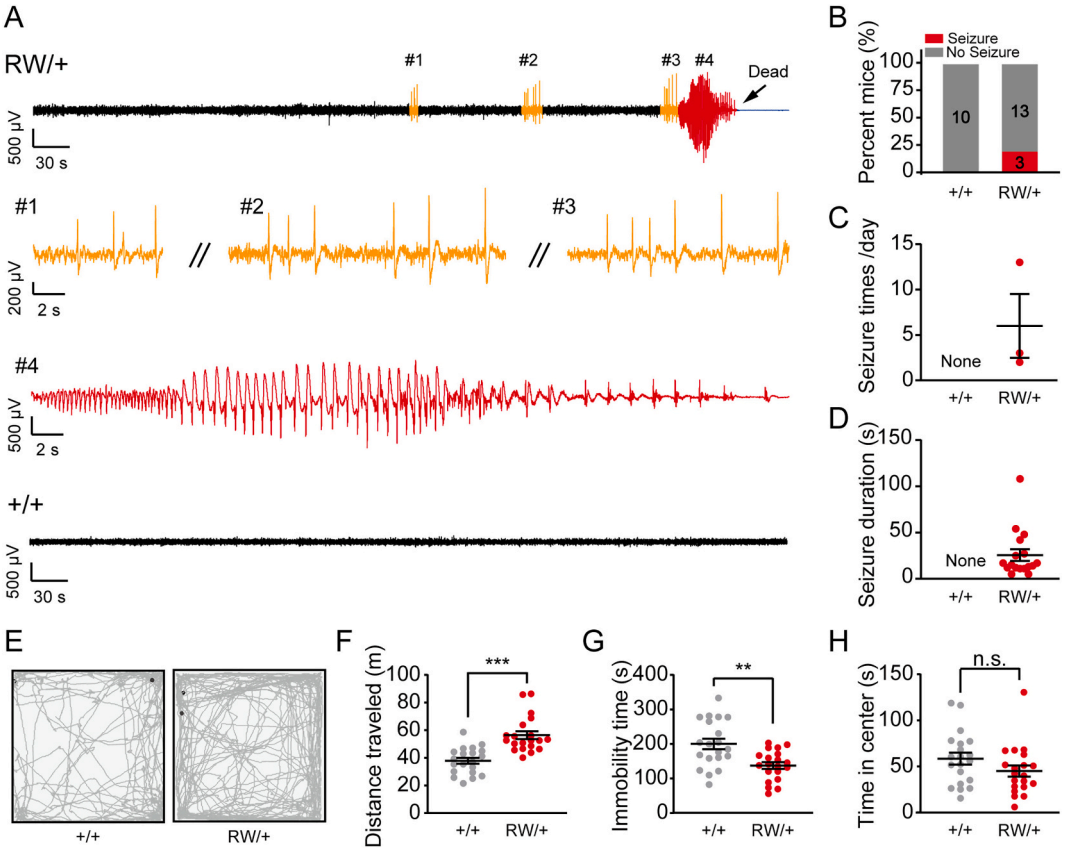

Fig. 3. Spontaneous seizures and hyperactivity in *Kcnq2*$^{RW/+}$ mice.
A) Representative ictal ECoG trace recordings from a *Kcnq2*$^{RW/+}$ mouse (upper panel) and normal ECoG trace from a *Kcnq2*$^{+/+}$ mice (bottom panel). B) The proportion with/without seizures in *Kcnq2*$^{RW/+}$ and *Kcnq2*$^{+/+}$ mice. C) Number of seizures per day and D) seizure duration of the three *Kcnq2*$^{RW/+}$ mice with spontaneous seizures. E) Representative locomotor traces of *Kcnq2*$^{RW/+}$ and *Kcnq2*$^{+/+}$ mice. Analysis of F) total distance, G) immobility time and H) time in center of *Kcnq2*$^{RW/+}$ and *Kcnq2*$^{+/+}$ mice in open field; $n = 12–20$ for each group.

$^{+}$ mice in chemoconvulsant-induced seizure susceptibility, pentylenetetrazole (PTZ) was used. At the dose of 60 mg/kg, 100% (12/12) *Kcnq2*$^{RW/+}$ mice exhibited GTCS, and 80% of them died within 1 h after PTZ injection, while only 50% (6/12) *Kcnq2*$^{+/+}$ mice exhibited GTCS and none of them died ($p = 0.0047$, Chi-square test); not all *Kcnq2*$^{+/+}$ mice displayed GTCS until an 100-mg/kg dose (Fig. 4G). In addition, seizures in *Kcnq2*$^{RW/+}$ mice were different from those occurring in *Kcnq2*$^{+/+}$ mice (Supplementary Videos 3, 4); as shown in Fig. 4H, seizures in *Kcnq2*$^{RW/+}$ mice more quickly shifted from stage III to stage V when compared to WT mice (50 mg/kg, $p = 0.0001$; 60 mg/kg, $p = 0.0013$, one-way ANOVA, Turkey's multiple comparison test), demonstrating a faster seizure progression due to increased epilepsy susceptibility in *Kcnq2*$^{RW/+}$ mice.

3.6. KCNQ2 openers attenuate drug- and electrically-induced seizures in *Kcnq2*$^{RW/+}$

According to the results described above, *Kcnq2*$^{RW/+}$ mice represent a valuable model to investigate the protective effects of ASMs against KCNQ2-related epilepsy; thus, the protective effects of HN37 and RTG against electrical 6-Hz, PTZ, and hyperthermia-induced seizures were investigated in *Kcnq2*$^{RW/+}$ mice.

The 6-Hz seizure model was performed with a stimulation current of 20 mA. Following HN37 treatment, the sensitivity of *Kcnq2*$^{RW/+}$ mice was dose-dependently reduced, with a higher potency than that of RTG (Fig. 5A); in fact, the EC_{50} of HN37 (6.9 mg/kg) was markedly lower than that of RTG (54.5 mg/kg). When the two drugs were compared in their ability to reduce seizure duration in the 6-Hz model, HN37 was found to decrease seizure duration at the dose of 5.6 mg/kg ($p = 0.0281$, one-way ANOVA, Dunnett's post test), while the first effective dose of RTG was 60 mg/kg ($p = 0.0047$, one-way ANOVA, Dunnett's post test) (Fig. 5B). These results demonstrated that HN37 effectively protected the *Kcnq2*$^{RW/+}$ mice against 6-Hz induced seizure, showing a roughly 10-times higher potency when compared to RTG.

The effects of HN37 and RTG were also investigated in PTZ-induced seizure in *Kcnq2*$^{RW/+}$ mice. Treatment with HN37 fully abolished GTCS at the dose of 10 mg/kg ($p < 0.0001$, Chi-square test); a higher dose of RTG (80 mg/kg) was needed to achieve the similar efficacy ($p = 0.0004$, Chi-square test) (Fig. 5C). In addition, HN37 decreased the seizure score at a dose of 10 mg/kg ($p < 0.0001$, Mann Whitney test), while a significant decrease was only observed for RTG at the dose of 80 mg/kg ($p = 0.0002$, Mann Whitney test) (Fig. 5D). These results demonstrate that HN37 protected *Kcnq2*$^{RW/+}$ mice against PTZ-induced seizure, showing higher potency when compared to RTG.

In addition to electrical 6-Hz and PTZ models, the effects of HN37 and RTG were also evaluated in *Kcnq2*$^{RW/+}$ mice subjected to the hyperthermia model, with seizure threshold temperature and duration used as evaluation criteria. The seizure threshold temperature was significantly elevated by HN37 at a dose of 10 mg/kg ($p < 0.0001$), while RTG doses of 40 mg/kg ($p = 0.0031$) or 80 mg/kg ($p = 0.0011$, one-way ANOVA, Dunnett's post test) were needed to achieve comparable effects. In addition, there was a nonsignificant seizure-latency prolongation trend after the application of HN37 at a dose of 10 mg/kg ($p = 0.1619$) or 5 mg/kg ($p = 0.8782$), or RTG at a dose of 40 mg/kg ($p = 0.2386$) or 80 mg/kg ($p = 0.2662$, one-way ANOVA, Dunnett's post test), although seizure latencies showed a tendency to increase. These results demonstrated that HN37 showed marked efficacy in preventing hyperthermia-induced seizures, also displaying higher potency when

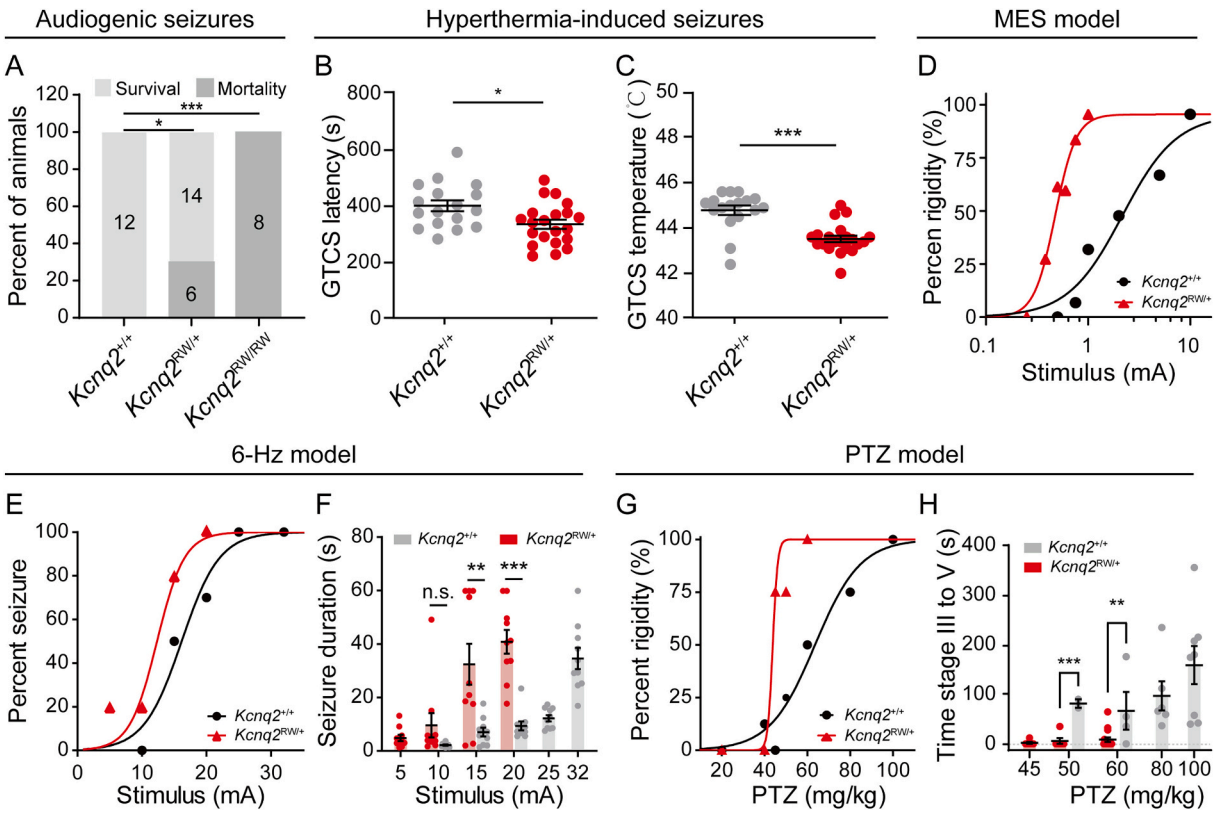

Fig. 4. *Kcnq2*$^{RW/+}$ mice exhibit reduced threshold to induced seizures.
A) The proportion with/without audiogenic seizures induced by a noise of 110 dB. B) The GTCS latency and C) temperature in hyperthermia-induced seizure test. D) Convulsive-current curves generated from MES model. E) Rigidity-current curves and F) seizure duration of *Kcnq2*$^{RW/+}$ and *Kcnq2*$^{+/+}$ mice in 6-Hz model. G) Rigidity-current curves and H) the time spent from stage III to stage V seizure of *Kcnq2*$^{RW/+}$ and WT mice in PTZ model. $n = 8–12$ for each group in above experiments; n.s. not significant, * $P < 0.05$, ** $P < 0.01$, $P < 0.001$ (Chi-square test for A; unpaired Student's *t*-test for B, C, F and H).

compared to RTG.

4. Discussion

Developing animal models reproducing at least some of the phenotypic features of human epilepsies is of critical importance for the understanding of their underlying pathophysiology and for developing novel and personalized treatment approaches. In the present work, we engineered a mouse line carrying the disease-causing *Kcnq2*-R207W variant as a novel model of KCNQ2-related epilepsy. While homozygous mice displayed a short lifespan, growth retardation, spontaneous seizures, and SUDEP, heterozygous mice showed incomplete penetrance of the spontaneous seizure phenotype and a reduced threshold to electrically-, thermally-, auditory-, and drug-induced seizures. Finally, we demonstrated that seizures induced in heterozygous mice were dramatically reduced after administration of a novel KCNQ opener HN37, with an approximately 10-times higher potency when compared to retigabine.

4.1. The first mouse line carrying a voltage-sensor mutation (R207W) in *Kcnq2*

In an attempt to investigate the possible contribution of KCNQ2-encoded potassium channel subunits to neuronal excitability underlying complex neuronal functions and to capture at least some of the phenotypes of KCNQ2-related epilepsies, several rodent models have been developed over the last two decades. In particular, the *Kcnq2*-KO and *Kcnq2*-G279S mice were constructed mainly for studying the physiological function of KCNQ2 since neither was based on mutant allele from patients (Peters et al., 2005; Watanabe et al., 2000). Similarly, Szt1 mice, which were obtained by random mutagenesis and carried a large deletion including the C-terminus of the Kcnq2 gene and two additional genes, display reduced seizure thresholds, thus providing important clues on the pathophysiological role of KCNQ2 subunits in seizure susceptibility (Yang et al., 2003). Notably, the lack of the C-terminus in KCNQ2 impairs the trafficking of the KCNQ2 subunit to the membrane (Chung et al., 2006); consequently, the Szt1 mouse is a better model for haploinsufficiency of the KCNQ2 subunit rather than dominant-negative KCNQ2 current suppression associated to more severe human phenotypes (Miceli et al., 2013; Orhan et al., 2014). The adult phenotype of Szt1 mice was similar to that of *Kcnq2*$^{A306T/+}$ and *Kcnq3*$^{G311V/+}$ heterozygous knock-in mice, carrying pore mutations in KCNQ2 or KCNQ3, respectively, both reproducing naturally-occurring variants found in SeLFNE families (Singh et al., 2008). These mice exhibited no spontaneous seizures but reduced thresholds to electrically induced seizures compared to wild-type littermate mice; by contrast, both *Kcnq2*$^{A306T/A306T}$ and *Kcnq3*$^{G311V/G311V}$ homozygous mutant mice exhibited early-onset spontaneous generalized tonic-clonic seizures which recurred into adulthood, not associated to hippocampal mossy fiber sprouting or neuronal loss. Thereafter, two other mouse models, *Kcnq2*-A306T and *Kcnq2*-Y284C mice, were developed using the kick-in mutational strategy, and homozygotes from both lines showed spontaneous seizures while heterozygotes were phenotypically indistinguishable from WT mice except for a reduced seizure threshold (Singh et al., 2008; Tomonoh et al., 2014), a result consistent with that of Singh et al. (Singh et al., 2008). Recently, a *Kcnq2*-T274M mouse model harboring a variant recurrently known to cause DEE7 was established, in which heterozygous mice in the 129Sv genetic background displayed spontaneous generalized seizures and cognitive impairment (Milh et al., 2020).

While it has been consistently demonstrated that missense human

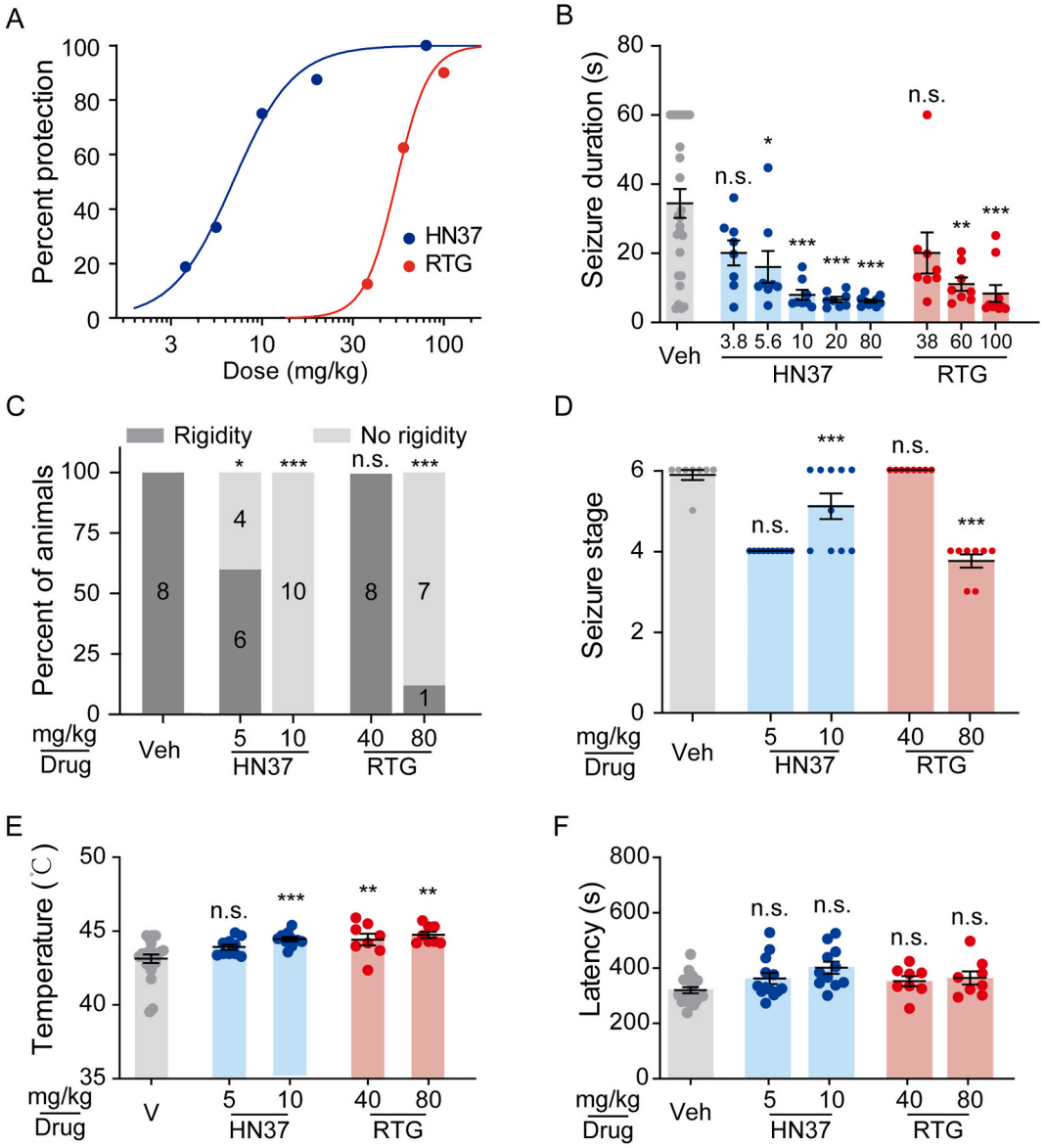

Fig. 5. HN37 protects *Kcnq2*$^{RW/+}$ mice against induced seizures.
A) Dose-response curves of HN37 and RTG for 6-Hz induced seizures in *Kcnq2*$^{RW/+}$ mice. B) Seizure duration in *Kcnq2*$^{RW/+}$ mice induced by 6-Hz after the application of drugs or vehicle. C) Proportion of rigidity and D) seizure stage in *Kcnq2*$^{RW/+}$ mice induced by PTZ after the application of drugs or vehicle. E) Seizure temperature and F) seizure latency in *Kcnq2*$^{RW/+}$ mice induced by hyperthermia after the application of drugs or vehicle. Mice were pretreated with test drug or vehicle and then received a PTZ, 6-Hz or hyperthermia stimulus; n = 8–12 for each group in above experiments; n.s. not significant, * $P < 0.05$, ** $P < 0.01$, $P < 0.001$ (Chi-square test for C; one-way ANOVA, Turkey test for B, D, E and F).

mutations found in patients with KCNQ2-related epilepsies are mainly located in hot spots, including the S4 voltage-sensor, the pore, and two calmodulin-binding helices (A and B) in the C-terminal region, existing knock-in mice modelling KCNQ2-related epilepsies only carry mutations in the pore domain, while no mouse model reproducing a voltage-sensor variant pathogenic in humans has been developed to our knowledge. Thus, our model is the first knock-in mice harboring a pathogenic mutation in the voltage sensor of *Kcnq2*.

4.2. The epileptic phenotypes in Kcnq2-R207W heterozygotes

Kcnq2-R207W homozygotes showed a high probability of premature death (Fig. 2B, C), which was also reported in the *Kcnq2*-A306T mice (Singh et al., 2008). It is likely that premature death is highly correlated with the mutant KCNQ2 function, as both the *Kcnq2*-knockout mice and homozygous mice harboring nonfunctional *Kcnq2*-T274M died at birth, while homozygous mice harboring *Kcnq2*-Y284C with mildly impaired function survived (Milh et al., 2020; Tomonoh et al., 2014; Watanabe et al., 2000). Consistent with this, the KCNQ2 channel function of R207W or A306T mutants was severely impaired but not completely disrupted, which may explain the incomplete penetrance of premature death(Singh et al., 2008; Tomonoh et al., 2014).

In adult *Kcnq2*-R207W heterozygotes, spontaneous seizures were only rarely observed in adult mice (9/64; 14%); technical difficulties in the continuous video–ECoG monitoring during the first weeks of life prevented a full description of the epilepsy phenotype at earlier (pre-weaning) developmental stages. Notably, both in self-limited and severe phenotypes of KCNQ2-related diseases, seizure frequency significantly decreases during development, and seizures are not present in most adults with neonatal-onset KCNQ2-DEE (Boets et al., 2022). Also in SeLFNE, the seizure recurrence risk in adult individuals from affected families is around 10% (Psenka and Holden, 1996). Both these

observations may explain the low penetrance of spontaneous seizures in adult heterozygous mice observed in our present work.

In patients carrying the KCNQ2-R07W variant, the seizure type manifests in various forms, mainly including myoclonus and convulsions with tonic and/or clonic features; at least some of these epilepsy phenotypes are captured in *Kcnq2*-R207W heterozygotes that displayed visible myoclonus and severe GTCS. In addition, *Kcnq2*-R207W heterozygotes displayed increased seizure susceptibility in multiple induced seizure tests. Thus, the *Kcnq2*-R207W heterozygote is a suitable model for the study of pathogenetic mechanisms and ASM discovery.

Notably, the induced seizure models do not adequately represent the phenotypes of patients with KCNQ2-related epilepsy in clinical, as these patients do not bear electrical or chemical stimulus physiologically. In addition, the body temperatures for hyperthermia-induced are higher relative to other febrile seizure models that have seizures between 40 and 42 °C (Dutton et al., 2013); the physiological relevance of this inducer is not clear despite the difference between genotypes. The incomplete penetrance of spontaneous seizures in adult *Kcnq2*-R207W heterozygotes also poses some limitations for the routine practical applicability of studies using these mice. It is well known that the genetic background exerts a major influence on seizure expressivity in mice; as an example, male mice carrying the *Kcnq3*-G311V mutation on the B6 background exhibited a threshold for partial psychomotor seizure no different from their wild-type littermates, but this mutation did significantly reduce the threshold of male mice carrying the same mutation on the FVB background (Otto et al., 2009). In addition, *Scn1a*$^{+/-}$ mice maintained on the 129S6/SvEvTac strain have no spontaneous seizures, while mating with C57BL/6 J results in epilepsy and premature lethality in their progeny.(Bergren et al., 2005; Ogiwara et al., 2007; Yu et al., 2006) Thus, maintaining the *Kcnq2*-R207W mice in a more susceptible genetic background like DBA/2 or SJL/J may be an effective approach to enhance the penetrance of spontaneous seizures in *Kcnq2*-R207W heterozygotes, a desired achievement needed to enhance the feasibility of studies in adult animals from this newly-developed mouse model.

4.3. KCNQ openers as reasonable options for KCNQ2-related epilepsy

In the clinic, sodium channel blockers appear as the preferred antiseizure medications (ASMs) for the treatment of KCNQ2-related epilepsies; in fact, seizures are usually controlled with phenobarbital or phenytoin in individuals with SeLFNE (Painter et al., 1981), and favorable responses to phenytoin or carbamazepine have been described in several studies of DEE7 patients resistant to various ASMs (Kato et al., 2013; Numis et al., 2014; Pisano et al., 2015; Weckhuysen et al., 2013; Weckhuysen et al., 2012). In addition, retigabine (RTG), a selective activator of KCNQ channels, was shown to revert the channel dysfunction caused by LOF variants when tested in vitro (Miceli et al., 2013; Xiong et al., 2007; Xiong et al., 2008). Retigabine also showed anticonvulsant efficacy in A306T and Y284 mice (Ihara et al., 2016) and was well tolerated and at least partially effective in children with KCNQ2-DEE when started early (Millichap et al., 2016; Weckhuysen et al., 2013) Although RTG has been withdrawn from the market mostly because of its side effects like skin discoloration, a proprietary pediatric formulation of RTG has received Orphan Drug Designation for the treatment of seizures associated with KCNQ2-DEE from both FDA and EMA, and a clinical trial with this formulation has been recently started (https://clinicaltrials.gov/ct2/show/NCT04639310).

The novel KCNQ opener HN37 displays improved potency towards KCNQ channels relative to RTG in electrophysiological studies in vitro, and an excellent efficacy against seizures in a series of preclinical models, leading to the beginning of clinical trials in China to investigate HN37 efficacy and safety as an anticonvulsant (Zhang et al., 2021). Moreover, HN37 possesses better chemical stability and brain distribution compared to RTG, likely resulting in reduced skin discoloration and other side effects (French et al., 2011). Considering the enhanced efficacy and the improved safety profile, HN37 may be a reasonable therapeutic option for precision treatment in KCNQ2-related epilepsy. In our present study, we tested the effects of HN37 on several models of induced seizures in *Kcnq2*-R207W heterozygotes in vivo and found that HN37 was capable of exerting a marked anticonvulsant effect, in each of them also displaying a more potent anticonvulsant activity when compared to RTG. A limitation needs to be stated was that we only used male mice only in this study; we took this strategy to avoid a larger variation in behavioral data, which would require fewer animal in each group to reach significant differences if present, but may also limit the generalizability of these findings. In addition, given the sub-optimal translation potential to humans of the pharmacological results obtained in induced seizure models, future experiments will be directed at evaluating the effects of ASMs on spontaneous epilepsy in heterozygous mice in which the *Kcnq2*-R207W genotype will be propagated in a more susceptible genetic background, therefore displaying an increased proportion of spontaneous seizure.

In conclusion, in the present work, we developed a *Kcnq2*-R207W mouse model, which appears to be a suitable model for KCNQ2-related epilepsy, and demonstrate that KCNQ openers are effective in preventing seizures in this model, highlighting their possible usefulness as precision medicines for KCNQ2-related epilepsies in humans.

Supplementary data to this article can be found online at https://doi.org/10.1016/j.nbd.2022.105860.

Conflict of interest

The authors have no financial conflicts of interest to disclose. We confirm that we have read the Journal's position on issues involved in ethical publication and affirm that this report is consistent with those guidelines.

Author contributions

FT, MT and ZG conceived and planned the experiments; FT, BC, HX and LZ carried out the experiments; FN and NL contributed to the interpretation of the results; FT, MT and ZG wrote the paper with input from all authors.

Data availability

No data was used for the research described in the article.

Acknowledgments

ZG received funding from the High-level new R&D institute (2019B090904008) and the High-level Innovative Research Institute (2021B0909050003) of the Department of Science and Technology of Guangdong Province, and the National Science Fund for Distinguished Young Scholars (81825021); FT received funding from the Public Welfare and Basic Research Project of Zhongshan City (210724194041939). MT received funding from the Italian Ministry for University and Research (MIUR) (PRIN 2017ALCR7C), the Italian Ministry of Health (Project RF-2019-12370491), the European Commission H2020 (UNICOM- 875299), and the European Joint Programme on Rare Disease JTC 2020 (TreatKCNQ).

References

Alberini, G., Benfenati, F., Maragliano, L., 2021. Structural mechanism of omega-currents in a mutated Kv7.2 voltage sensor domain from molecular dynamics simulations. J. Chem. Inf. Model. 61, 1354–1367. https://doi.org/10.1021/acs.jcim.0c01407.

Bergren, S.K., Chen, S., Galecki, A., Kearney, J.A., 2005. Genetic modifiers affecting severity of epilepsy caused by mutation of sodium channel Scn2a. Mamm. Genom. 16, 683–690. https://doi.org/10.1007/s00335-005-0049-4.

Biervert, C., Schroeder, B.C., Kubisch, C., Berkovic, S.F., Propping, P., Jentsch, T.J., Steinlein, O.K., 1998. A potassium channel mutation in neonatal human epilepsy. Science 279, 403–406. https://doi.org/10.1126/science.279.5349.403.

Blumkin, L., Suls, A., Deconinck, T., De Jonghe, P., Linder, I., Kivity, S., Dabby, R., Leshinsky-Silver, E., Lev, D., Lerman-Sagie, T., 2012. Neonatal seizures associated with a severe neonatal myoclonus like dyskinesia due to a familial KCNQ2 gene mutation. Eur. J. Paediatr. Neurol. 16, 356–360. https://doi.org/10.1016/j.ejpn.2011.11.004.

Boets, S., Johannesen, K.M., Destree, A., Manti, F., Ramantani, G., Lesca, G., Vercueil, L., Koenig, M.K., Striano, P., Moller, R.S., et al., 2022. Adult phenotype of KCNQ2 encephalopathy. J. Med. Genet. 59, 528–535. https://doi.org/10.1136/jmedgenet-2020-107449.

Brown, D.A., Adams, P.R., 1980. Muscarinic suppression of a novel voltage-sensitive K+ current in a vertebrate neurone. Nature 283, 673–676. https://doi.org/10.1038/283673a0.

Chung, H.J., Jan, Y.N., Jan, L.Y., 2006. Polarized axonal surface expression of neuronal KCNQ channels is mediated by multiple signals in the KCNQ2 and KCNQ3 C-terminal domains. Proc. Natl. Acad. Sci. U. S. A. 103, 8870–8875. https://doi.org/10.1073/pnas.0603376103.

Dedek, K., Kunath, B., Kananura, C., Reuner, U., Jentsch, T.J., Steinlein, O.K., 2001. Myokymia and neonatal epilepsy caused by a mutation in the voltage sensor of the KCNQ2 K+ channel. Proc. Natl. Acad. Sci. U. S. A. 98, 12272–12277. https://doi.org/10.1073/pnas.211431298.

Dhamija, R., Goodkin, H.P., Bailey, R., Chambers, C., Brenton, J.N., 2017. A case of KCNQ2-associated movement disorder triggered by fever. J. Child Neurol. 32, 1123–1124. https://doi.org/10.1177/0883073817736702.

Dutton, S.B., Makinson, C.D., Papale, L.A., Shankar, A., Balakrishnan, B., Nakazawa, K., Escayg, A., 2013. Preferential inactivation of Scn1a in parvalbumin interneurons increases seizure susceptibility. Neurobiol. Dis. 49, 211–220. https://doi.org/10.1016/j.nbd.2012.08.012.

French, J.A., Abou-Khalil, B.W., Leroy, R.F., Yacubian, E.M., Shin, P., Hall, S., Mansbach, H., Nohria, V., Investigators, R.S., 2011. Randomized, double-blind, placebo-controlled trial of ezogabine (retigabine) in partial epilepsy. Neurology 76, 1555–1563. https://doi.org/10.1212/WNL.0b013e3182194bd3.

Ihara, Y., Tomonoh, Y., Deshimaru, M., Zhang, B., Uchida, T., Ishii, A., Hirose, S., 2016. Retigabine, a Kv7.2/Kv7.3-channel opener, attenuates drug-induced seizures in Knock-in mice harboring Kcnq2 mutations. PLoS One 11, e0150095. https://doi.org/10.1371/journal.pone.0150095.

Kato, M., Yamagata, T., Kubota, M., Arai, H., Yamashita, S., Nakagawa, T., Fujii, T., Sugai, K., Imai, K., Uster, T., et al., 2013. Clinical spectrum of early onset epileptic encephalopathies caused by KCNQ2 mutation. Epilepsia 54, 1282–1287. https://doi.org/10.1111/epi.12200.

Martire, M., Castaldo, P., D'Amico, M., Preziosi, P., Annunziato, L., Taglialatela, M., 2004. M channels containing KCNQ2 subunits modulate norepinephrine, aspartate, and GABA release from hippocampal nerve terminals. J. Neurosci. 24, 592–597. https://doi.org/10.1523/JNEUROSCI.3143-03.2004.

Miceli, F., Soldovieri, M.V., Hernandez, C.C., Shapiro, M.S., Annunziato, L., Taglialatela, M., 2008. Gating consequences of charge neutralization of arginine residues in the S4 segment of K(v)7.2, an epilepsy-linked K+ channel subunit. Biophys. J. 95, 2254–2264. https://doi.org/10.1529/biophysj.107.128371.

Miceli, F., Soldovieri, M.V., Joshi, N., Weckhuysen, S., Cooper, E., and Taglialatela, M. (2010). KCNQ2-related disorders. In GeneReviews((R)), M.P. Adam, H.H. Ardinger, R.A. Pagon, S.E. Wallace, L.J.H. Bean, K. Stephens, and A. Amemiya, eds. (Seattle (WA)).

Miceli, F., Vargas, E., Bezanilla, F., Taglialatela, M., 2012. Gating currents from Kv7 channels carrying neuronal hyperexcitability mutations in the voltage-sensing domain. Biophys. J. 102, 1372–1382. https://doi.org/10.1016/j.bpj.2012.02.004.

Miceli, F., Soldovieri, M.V., Ambrosino, P., Barrese, V., Migliore, M., Cilio, M.R., Taglialatela, M., 2013. Genotype-phenotype correlations in neonatal epilepsies caused by mutations in the voltage sensor of K(v)7.2 potassium channel subunits. Proc. Natl. Acad. Sci. U. S. A. 110, 4386–4391. https://doi.org/10.1073/pnas.1216867110.

Milh, M., Roubertoux, P., Biba, N., Chavany, J., Spiga Ghata, A., Fulachier, C., Collins, S. C., Wagner, C., Roux, J.C., Yalcin, B., et al., 2020. A knock-in mouse model for KCNQ2-related epileptic encephalopathy displays spontaneous generalized seizures and cognitive impairment. Epilepsia 61, 868–878. https://doi.org/10.1111/epi.16494.

Millichap, J.J., Park, K.L., Tsuchida, T., Ben-Zeev, B., Carmant, L., Flamini, R., Joshi, N., Levisohn, P.M., Marsh, E., Nangia, S., et al., 2016. KCNQ2 encephalopathy: features, mutational hot spots, and ezogabine treatment of 11 patients. Neurol. Genet. 2, e96 https://doi.org/10.1212/NXG.0000000000000096.

Numis, A.L., Angriman, M., Sullivan, J.E., Lewis, A.J., Striano, P., Nabbout, R., Cilio, M. R., 2014. KCNQ2 encephalopathy: delineation of the electroclinical phenotype and treatment response. Neurology 82, 368–370. https://doi.org/10.1212/WNL.0000000000000060.

Ogiwara, I., Miyamoto, H., Morita, N., Atapour, N., Mazaki, E., Inoue, I., Takeuchi, T., Itohara, S., Yanagawa, Y., Obata, K., et al., 2007. Nav1.1 localizes to axons of parvalbumin-positive inhibitory interneurons: a circuit basis for epileptic seizures in mice carrying an Scn1a gene mutation. J. Neurosci. 27, 5903–5914. https://doi.org/10.1523/JNEUROSCI.5270-06.2007.

Orhan, G., Bock, M., Schepers, D., Ilina, E.I., Reichel, S.N., Loffler, H., Jezutkovic, N., Weckhuysen, S., Mandelstam, S., Suls, A., et al., 2014. Dominant-negative effects of KCNQ2 mutations are associated with epileptic encephalopathy. Ann. Neurol. 75, 382–394. https://doi.org/10.1002/ana.24080.

Otto, J.F., Singh, N.A., Dahle, E.J., Leppert, M.F., Pappas, C.M., Pruess, T.H., Wilcox, K. S., White, H.S., 2009. Electroconvulsive seizure thresholds and kindling acquisition rates are altered in mouse models of human KCNQ2 and KCNQ3 mutations for benign familial neonatal convulsions. Epilepsia 50, 1752–1759. https://doi.org/10.1111/j.1528-1167.2009.02100.x.

Painter, M.J., Pippenger, C., Wasterlain, C., Barmada, M., Pitlick, W., Carter, G., Abern, S., 1981. Phenobarbital and phenytoin in neonatal seizures: metabolism and tissue distribution. Neurology 31, 1107–1112. https://doi.org/10.1212/wnl.31.9.1107.

Peters, H.C., Hu, H., Pongs, O., Storm, J.F., Isbrandt, D., 2005. Conditional transgenic suppression of M channels in mouse brain reveals functions in neuronal excitability, resonance and behavior. Nat. Neurosci. 8, 51–60. https://doi.org/10.1038/nn1375.

Pisano, T., Numis, A.L., Heavin, S.B., Weckhuysen, S., Angriman, M., Suls, A., Podesta, B., Thibert, R.L., Shapiro, K.A., Guerrini, R., et al., 2015. Early and effective treatment of KCNQ2 encephalopathy. Epilepsia 56, 685–691. https://doi.org/10.1111/epi.12984.

Psenka, T.M., Holden, K.R., 1996. Benign familial neonatal convulsions; psychosocial adjustment to the threat of recurrent seizures. Seizure 5, 243–245. https://doi.org/10.1016/s1059-1311(96)80044-6.

Singh, N.A., Charlier, C., Stauffer, D., DuPont, B.R., Leach, R.J., Melis, R., Ronen, G.M., Bjerre, I., Quattlebaum, T., Murphy, J.V., et al., 1998. A novel potassium channel gene, KCNQ2, is mutated in an inherited epilepsy of newborns. Nat. Genet. 18, 25–29. https://doi.org/10.1038/ng0198-25.

Singh, N.A., Otto, J.F., Dahle, E.J., Pappas, C., Leslie, J.D., Vilaythong, A., Noebels, J.L., White, H.S., Wilcox, K.S., Leppert, M.F., 2008. Mouse models of human KCNQ2 and KCNQ3 mutations for benign familial neonatal convulsions show seizures and neuronal plasticity without synaptic reorganization. J. Physiol. 586, 3405–3423. https://doi.org/10.1113/jphysiol.2008.154971.

Soldovieri, M.V., Boutry-Kryza, N., Milh, M., Doummar, D., Heron, B., Bourel, E., Ambrosino, P., Miceli, F., De Maria, M., Dorison, N., et al., 2014. Novel KCNQ2 and KCNQ3 mutations in a large cohort of families with benign neonatal epilepsy: first evidence for an altered channel regulation by syntaxin-1A. Hum. Mutat. 35, 356–367. https://doi.org/10.1002/humu.22500.

Symonds, J.D., Zuberi, S.M., Stewart, K., McLellan, A., O'Regan, M., MacLeod, S., Jollands, A., Joss, S., Kirkpatrick, M., Brunklaus, A., et al., 2019. Incidence and phenotypes of childhood-onset genetic epilepsies: a prospective population-based national cohort. Brain 142, 2303–2318. https://doi.org/10.1093/brain/awz195.

Tomonoh, Y., Deshimaru, M., Araki, K., Miyazaki, Y., Arasaki, T., Tanaka, Y., Kitamura, H., Mori, F., Wakabayashi, K., Yamashita, S., et al., 2014. The kick-in system: a novel rapid knock-in strategy. PLoS One 9, e88549. https://doi.org/10.1371/journal.pone.0088549.

Uchida, T., Lossin, C., Ihara, Y., Deshimaru, M., Yanagawa, Y., Koyama, S., Hirose, S., 2017. Abnormal gamma-aminobutyric acid neurotransmission in a Kcnq2 model of early onset epilepsy. Epilepsia 58, 1430–1439. https://doi.org/10.1111/epi.13807.

Watanabe, H., Nagata, E., Kosakai, A., Nakamura, M., Yokoyama, M., Tanaka, K., Sasai, H., 2000. Disruption of the epilepsy KCNQ2 gene results in neural hyperexcitability. J. Neurochem. 75, 28–33. https://doi.org/10.1046/j.1471-4159.2000.0750028.x.

Weckhuysen, S., Mandelstam, S., Suls, A., Audenaert, D., Deconinck, T., Claes, L.R., Deprez, L., Smets, K., Hristova, D., Yordanova, I., et al., 2012. KCNQ2 encephalopathy: emerging phenotype of a neonatal epileptic encephalopathy. Ann. Neurol. 71, 15–25. https://doi.org/10.1002/ana.22644.

Weckhuysen, S., Ivanovic, V., Hendrickx, R., Van Coster, R., Hjalgrim, H., Moller, R.S., Gronborg, S., Schoonjans, A.S., Ceulemans, B., Heavin, S.B., et al., 2013. Extending the KCNQ2 encephalopathy spectrum: clinical and neuroimaging findings in 17 patients. Neurology 81, 1697–1703. https://doi.org/10.1212/01.wnl.0000435296.72400.a1.

Xiong, Q., Sun, H., Li, M., 2007. Zinc pyrithione-mediated activation of voltage-gated KCNQ potassium channels rescues epileptogenic mutants. Nat. Chem. Biol. 3, 287–296. https://doi.org/10.1038/nchembio874.

Xiong, Q., Sun, H., Zhang, Y., Nan, F., Li, M., 2008. Combinatorial augmentation of voltage-gated KCNQ potassium channels by chemical openers. Proc. Natl. Acad. Sci. U. S. A. 105, 3128–3133. https://doi.org/10.1073/pnas.0712256105.

Yang, Y., Beyer, B.J., Otto, J.F., O'Brien, T.P., Letts, V.A., White, H.S., Frankel, W.N., 2003. Spontaneous deletion of epilepsy gene orthologs in a mutant mouse with a low electroconvulsive threshold. Hum. Mol. Genet. 12, 975–984. https://doi.org/10.1093/hmg/ddg118.

Yu, F.H., Mantegazza, M., Westenbroek, R.E., Robbins, C.A., Kalume, F., Burton, K.A., Spain, W.J., McKnight, G.S., Scheuer, T., Catterall, W.A., 2006. Reduced sodium current in GABAergic interneurons in a mouse model of severe myoclonic epilepsy in infancy. Nat. Neurosci. 9, 1142–1149. https://doi.org/10.1038/nn1754.

Zhang, Y.M., Xu, H.Y., Hu, H.N., Tian, F.Y., Chen, F., Liu, H.N., Zhan, L., Pi, X.P., Liu, J., Gao, Z.B., et al., 2021. Discovery of HN37 as a potent and chemically stable antiepileptic drug candidate. J. Med. Chem. 64, 5816–5837. https://doi.org/10.1021/acs.jmedchem.0c02252.